Supplementary Information for

Plasmon excitation in graphene nanoribbon arrays on SiC

Anastasiia A. Kniazeva[1 †], Samvel R. Yegian[1], Sergey A. Dyakov[1], Andrey V. Muratov[2], Denis M. Zhigunov[1], Oleg A. Klimenko[1, 2], Nikolay A. Gippius[1], and Vladimir N. Antonov[1]

[1] Skolkovo Institute of Science and Technology, Bolshoy Boulevard 30, bld. 1, Moscow, Russia

[2] PN Lebedev Physical Institute of RAS, Leninskiy prospekt 53, Moscow, Russia 119991

Correspondence to: Anastasiia Kniazeva: Anastasiya.Knyazeva@skoltech.ru

1 Plasmon Resonance dependence on Graphene Nanoribbon Array Width

The quasi-static scaling law is fairly good for GNR on SiO_2 substrate. The only parameter in the FFM model, which changes when SiO_2 is replaced with SiC, is the dielectric constant, ~4 for SiO_2 and ~10 for SiC. In the model high dielectric constant weakens sensitivity to the ribbon width.

To evaluate which aspect of the model primarily leads to the weakened dependence of the plasmon resonance frequency on ribbon width. We have investigated this question systematically, as described below.

First, we considered whether the frequency dispersion of the substrate permittivity might be responsible. Over the spectral range of interest (50-350 cm^{-1}), the permittivity of SiC varies more slowly than that of SiO_2. If dispersion were the dominant factor, one would expect a weaker width dependence for ribbons on SiC compared to SiO_2.

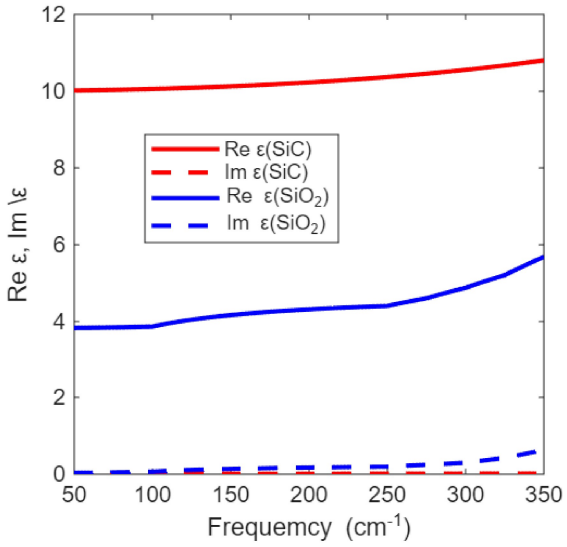

Fig. S1. Permittivity of SiC (red) and SiO_2 (blue).

To test this hypothesis, we calculated extinction spectra for four substrate materials with decreasing dielectric permittivity: SiC ($\varepsilon \approx 10$), a hypothetical dielectric with $\varepsilon \approx 8$, SiO_2 ($\varepsilon \approx 4$), and air ($\varepsilon = 1$). The results show that as the substrate permittivity decreases, the linewidth increases, the extinction maximum increases, and importantly, the dependence of the peak position on ribbon width becomes stronger. This indicates that the average permittivity of the substrate, not its frequency dispersion, is the key factor governing the width dependence.

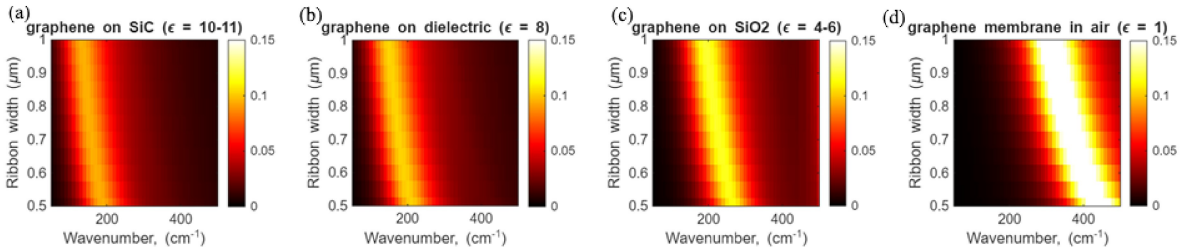

Fig. S2. Dependence of the peak position ($1-T_{GNR}/T_{sub}$) of graphene (E_F=250 meV, Γ= 15 meV) on (a) SiC (ε = 10-11), (b) dielectric (ε = 8), (c) SiO_2 (ε = 4-6), (d) in air (ε = 1) .

Next, to determine whether the ribbon width or the period affects the peak position, we performed two sets of simulations: varying the width while keeping the period constant, and varying the period while keeping the width constant. As one can see from Fig. S2, the peak position does not change when the period is varied at constant width, but shifts significantly when the width is varied at constant period. This demonstrates that the peak position is dominated by the ribbon width itself, and that localized plasmons on adjacent ribbons interact only weakly.

To explain why the width dependence is stronger for lower-index substrates, we examine the plasmon mode profile (Fig.5 from the main text).

This same observation explains why the extinction is higher for lower-index substrates: the field intensity within the absorbing graphene ribbon is greater when the substrate index is low, resulting in stronger light-matter interaction.

Finally, to confirm that the interaction between the two hot spots within the same ribbon is indeed the relevant mechanism, we calculated extinction spectra for ribbon widths up to 2 μm. At such large widths, the two edge hot spots are far apart and their overlap becomes negligible. Consequently, the dependence of the peak position on ribbon width becomes weakest, exactly as observed in the graph.

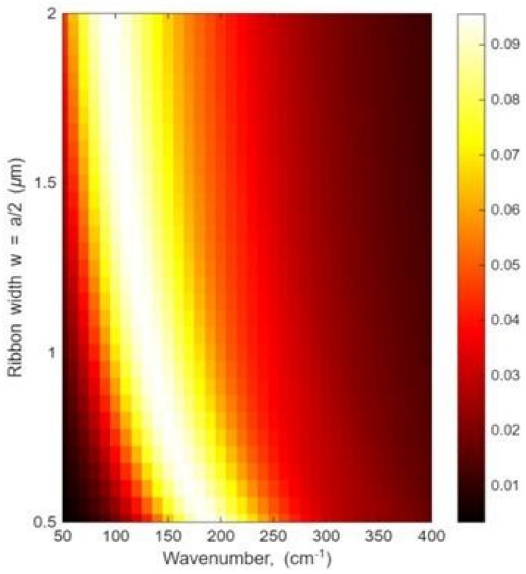

Fig. S3.Dependence of the GNRs on SiC plasmon extinction peak position on ribbon width, w, for wider widths range. E_F=250 meV, Γ=15 meV, w=a/2.

In summary, the weakened width dependence for higher-index substrates arises from reduced overlap between the two edge-localized hot spots due to stronger field confinement. The average substrate permittivity, not its frequency dispersion, is the controlling parameter, and inter-ribbon coupling plays a negligible role.

2 Harmonic Convergence in FMM Simulations

Starting with 30 harmonics the position of the peak doesn't depend on the number of harmonics, so 100 harmonics are enough for correct calculation of the extinction peak.

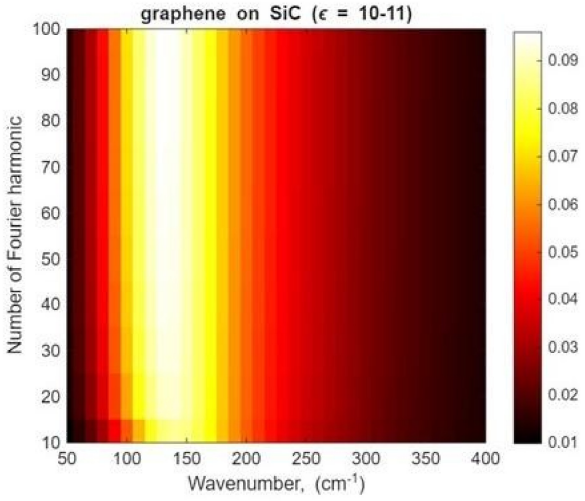

Fig. S4. Dependence of the extinction spectrum of GNR on SiC substrate on the number of Fourier harmonics.

3 Effect of Assumed Graphene Thickness in Fourier Modal Method Calculations

Surface conductivity and dielectric permittivity approaches for graphene treatment in electromagnetic simulations are equivalent since the following conditions are satisfied:
a) graphene film thickness is much smaller than wavelength (our wavelength range 25-65 um, while graphene thickness in our simulations is 0.3 nm);
b) fields do not vary significantly over the graphene film thickness;
c) we are not resolving atomic-scale effects.
To see the sensitivity of the calculated plasmon resonances to the assumed graphene thickness (d = 0.3 nm), and the influence of this parameter influence on the observed width dependence, we calculate the extinction spectrum of graphene nanoribbons for different d varied between 10^{-2} up to 10^{2} nm .

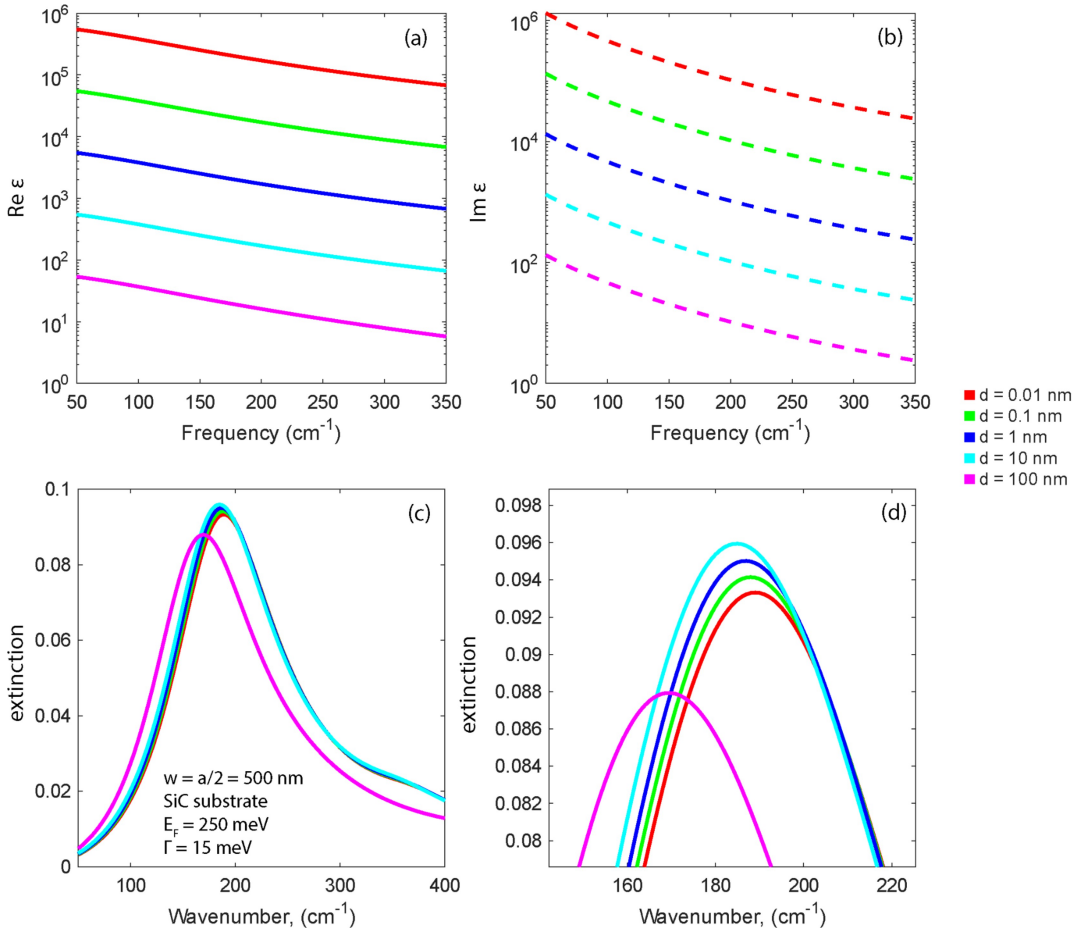

Fig.S5. Spectral dependence of (a) real and (b) imaginary parts of permittivity and (c) extinction of graphene film in respect to thickness of the film. (d) Zoomed in part of (c).

From these graphs one can see that while the effective dielectric permittivity of graphene film changes significantly with the increase of d from 0.01 to 100 nm, the resulting extinction spectrum remains almost independent on d up to d=~10 nm. At larger d, the phase retardation on graphene film thicknesses comes into play, and the output spectrum differs from those obtained at smaller d.

Please note that in our calculations made by the Fourier modal method, we do not introduce an effective dielectric permittivity of the GNR layer. Instead, we treat the GNR layer as a periodic one, where graphene ribbons have permittivity of graphene and the space between ribbons is characterized by the permittivity of air.

4 Scattering rate effect on plasmon extinction

To determine whether radiative scattering or intrinsic material losses dominate the observed plasmon linewidths, we performed extinction simulations for graphene ribbons with Γ = 0 and Γ = 15 meV.

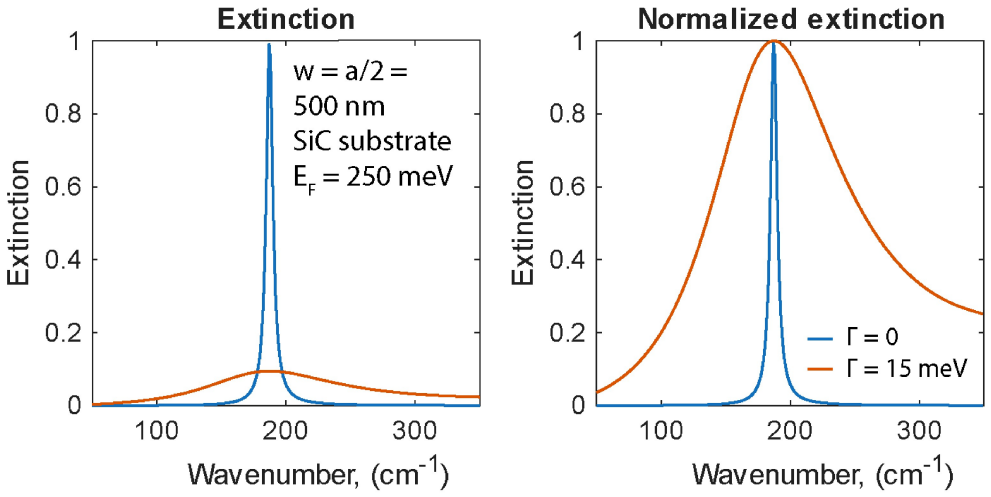

Fig. S6. Extinction simulations for graphene ribbons w=500 nm with Γ=0 (blue) meV and Γ=15 (orange) meV.

As one can see from Fig. S6, reducing Γ to zero significantly narrows the resonance linewidth, indicating that radiative losses are the primary contributor. While our simulations do not distinguish between edge scattering and far-field radiative scattering, the comparison between material and total linewidth already shows that radiative damping dominates.

The experimental and simulated results do not provide conclusive evidence for a width-dependent damping coefficient. Thus, our conclusions hold, regardless of whether such a dependence exists.

5 Inter- and intraband conductivity and permittivity

Clearly, in the presented frequency range, the intraband conductivity (Solid lines on Fig.S7) is dominant in comparison to the interband conductivity (Dashed lines).

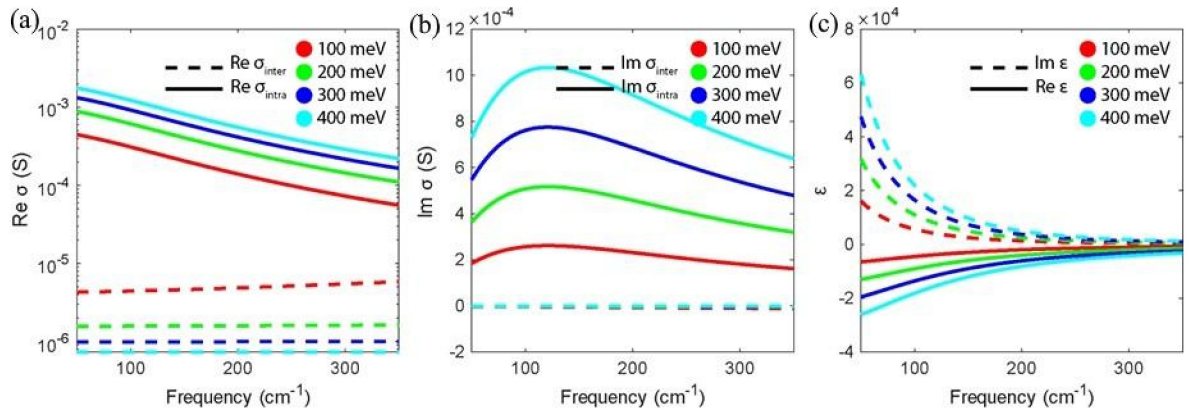

Fig. S7. Dependence of (a) real and (b) imaginary part of interband and intraband conductivity and (c) dependence of permittivity on the Fermi level.

6 Spectral properties of surface phonon-polaritons in graphene on SiC and on SiO_2

In order to compare the spectral positions of surface phonon polaritons (SPhPs) in SiC and SiO_2 with those of graphene plasmon resonances, we we plotted in the energy / in-plane k-vector coordinate system: (1) the norm of the scattering matrix, (2) the transmission through periodic and homogeneous graphene, and (3) the extinction. The frequency range of these plots covers both SPhP and plasmon excitations. On top of these figures, we superimposed the air, SiC, and SiO_2 light lines. From these plots, one can clearly see that the graphene plasmons in our study lie in the range of 200-300 cm^{-1} (yellow region in "Extinction" panel), whereas SPhPs in SiC appear at 800-950 cm^{-1}, and SPhPs in SiO_2 at around 500 cm^{-1} (closest approach of SiC and SiO_2 light lines (magenta curves) to k=0). Therefore, the results presented in our manuscript are related exclusively to graphene localized plasmons, with no spectral overlap or strong coupling with substrate SPhPs. Consequently, the observed deviation from the canonical analytical model is not due to phonon-plasmon hybridization.

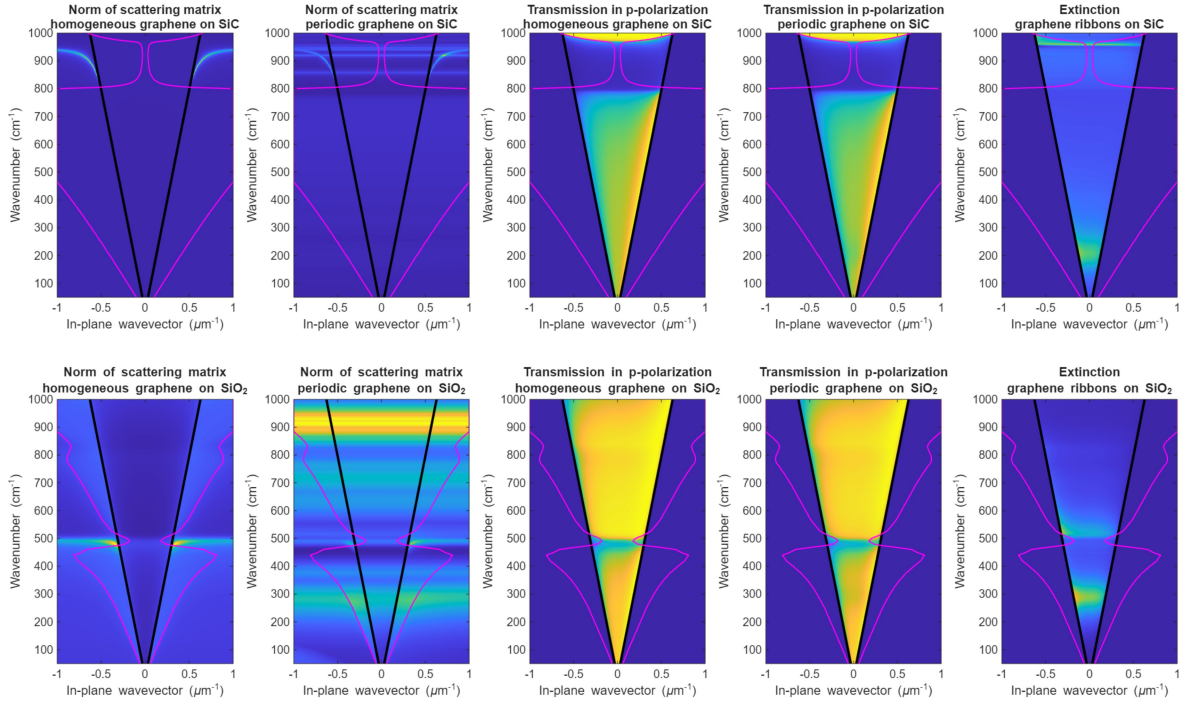

Fig. S8. The norm of the scattering matrix, the transmission through periodic and homogeneous graphene, and the extinction in the energy / in-plane k-vector coordinate system for graphene on SiC (upper row) and on SiO_2 (bottom row): light dispersion (black),surface phonon polariton graph (magenta).

7 Tunability of plasmon resonance in GNR arrays

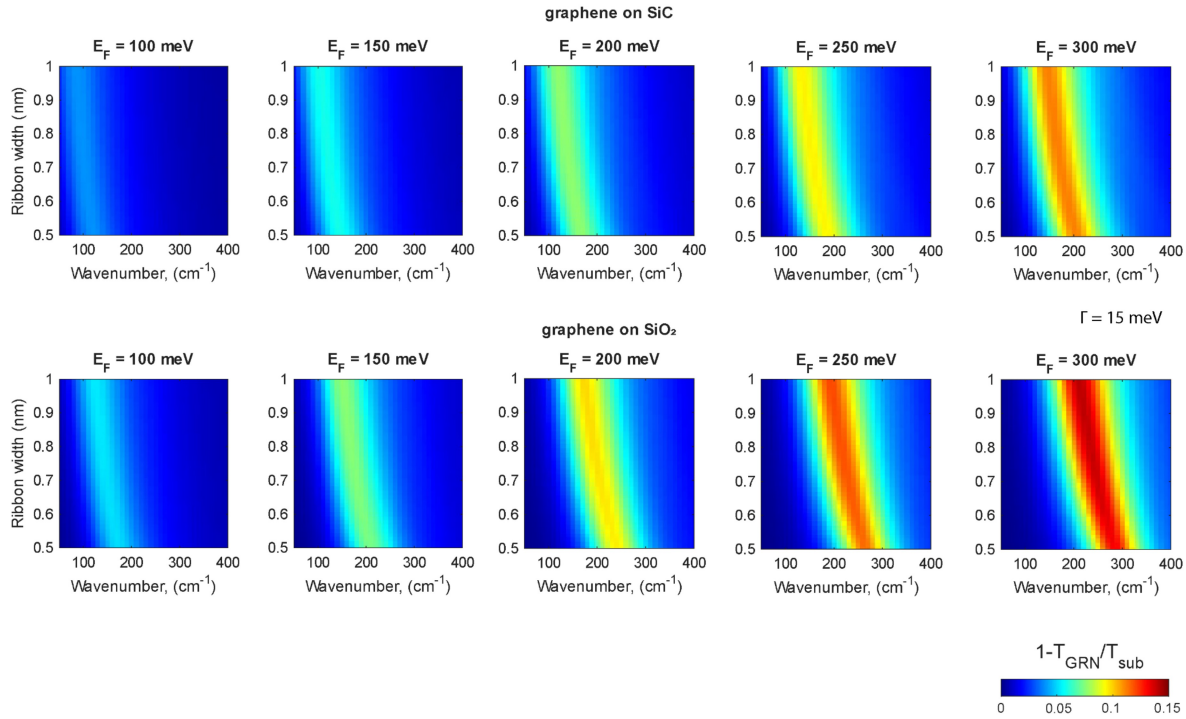

Fig. S9. Extinction spectra of GNR on SiC (upper row) and on SiO_2 (bottom row) calculated for different Fermi levels, Γ=15 meV, T=300 K. The color coding is shown below.